

Research Article

On the mechanism of inhibition of p27 degradation by 15-deoxy- $\Delta^{12,14}$ -prostaglandin J₂ in lymphoblasts of Alzheimer's disease patients

Ú. Muñoz^a, F. Bartolomé^a, N. Esteras^a, F. Bermejo-Pareja^{b,c} and Á. Martín-Requero^{a,d,*}

^a Department of Cellular and Molecular Pathophysiology, Centro de Investigaciones Biológicas (CSIC), Ramiro de Maeztu 9, 28040 Madrid (Spain), Fax: +34-91-536-0432, e-mail: amrequero@cib.csic.es

^b Hospital Doce de Octubre, Cra de Andalucía s/n, 28041 Madrid (Spain)

^c Centro de Investigación Biomédica en Red de Enfermedades Neurodegenerativas (CIBERNED) (Spain)

^d Centro de Investigación Biomédica en Red de Enfermedades Raras (CIBERER) (Spain)

Received 14 July 2008; received after revision 2 September 2008; accepted 12 September 2008

Online First 27 September 2008

Abstract. It has been proposed that neuroinflammation, among other factors, may trigger an aberrant neuronal cell cycle re-entry leading to neuronal death. Cell cycle disturbances are also detectable in peripheral cells from Alzheimer's disease (AD) patients. We previously reported that the anti-inflammatory 15-deoxy- $\Delta^{12,14}$ -prostaglandin J₂ (15d-PGJ₂) increased the cellular content of the cyclin-dependent kinase inhibitor p27, in lymphoblasts from AD patients. This work aimed at elucidating the mechanisms of 15d-PGJ₂-induced p27 accumulation. Phosphorylation, half-life, and the nucleo-cytoplasmic traffic of p27

protein were altered by 15d-PGJ₂ by mechanisms dependent on PI3K/Akt activity. 15d-PGJ₂ prevents the calmodulin-dependent Akt overactivation in AD lymphoblasts by blocking its binding to the 85-kDa regulatory subunit of PI3K. These effects of 15d-PGJ₂ were not mimicked by 9,10-dihydro-15-deoxy- $\Delta^{12,14}$ -prostaglandin J₂, suggesting that 15d-PGJ₂ acts independently of peroxisome proliferator-activated receptor γ activation and that the α,β -unsaturated carbonyl group in the cyclopentenone ring of 15d-PGJ₂ is a requisite for the observed effects.

Keywords. Alzheimer's disease, lymphocytes, cell proliferation, p27, proteasome activity, PI3K/Akt, cyclopentenone prostaglandins, Ca²⁺/calmodulin.

Introduction

Alzheimer's disease (AD) is a complex disorder afflicting the rapidly growing elderly segment of today's population, for which the current therapeutic tools offer only moderate symptomatic relief.

The AD brain pathophysiology includes not only the deposition of amyloid- β -protein, and neurofibrillary tangles but also, among other aspects, signs of chronic inflammation associated with significant neuronal loss [1]. Epidemiological studies have shown that long-term use of non-steroidal anti-inflammatory drugs (NSAIDs) reduces the risk of developing AD and delays its onset [2]. NSAIDs are known as ligands for the peroxisome proliferator-activated receptor γ (PPAR γ) [3], and it is believed that some of their

* Corresponding author.

effects are exerted through the activation of this transcription factor. Several natural and synthetic ligands for PPAR γ have been described, among them, 15-deoxy- $\Delta^{12,14}$ -prostaglandin J₂ (15d-PGJ₂), a prostaglandin J₂ metabolite, has been shown to be the most potent activator. 15d-PGJ₂ is known to increase in the course of inflammatory processes [4]. 15d-PGJ₂ displays anti-inflammatory and protective effects against certain types of injury in cellular systems, animal models and humans [5–7]. In addition to these effects, 15d-PGJ₂ has been shown to induce cell growth arrest and apoptosis in several cancer cell types [8, 9].

Research over the last decade has revealed that cell cycle-related events occur in susceptible neurons during AD, and that they are followed by apoptotic cell death [10–12]. Thus, understanding the molecular pathways underlying this cell cycle-mediated neurodegeneration may be important to find new therapeutic targets to slow or prevent the onset and progression of AD [13]. Several factors, including neuroinflammation can trigger aberrant neuronal cell cycle re-entry [14]. Therefore, it was hypothesized that the protective effects of NSAIDs in AD could be due not only to their ability to down-regulate the proinflammatory cytokines released by microglia, but also to their anti-proliferative effects [15, 16].

Numerous observations indicate that, while the predominant clinical expression arises from brain pathology, AD has systemic expression at the cellular and molecular levels [17, 18]. Although these alterations appear to have no consequences outside the central nervous system, their parallel expression in the brain could be considered a plausible pathophysiological model to explain partly the clinical manifestations. Of particular relevance to this work is the fact that cell cycle abnormalities are also found in peripheral cells from AD patients [19, 20].

Epstein Barr virus (EBV) infection *in vitro* causes transformation of B cells and generates B lymphoblastoid cell lines (LCLs) [21]. These LCLs retain the phenotype and functions of mature B cells [22]. LCLs have been widely used as models in various biological and medical studies [23]. Previous work from this laboratory, using EBV-immortalized lymphocytes from late-onset AD patients, demonstrated a Ca²⁺/calmodulin (CaM)-dependent stimulation of cell proliferation and survival of AD lymphoblasts compared with age-matched non-demented donors [24, 25]. Moreover, we reported that immortalization of peripheral lymphocytes from AD patients with the Epstein Barr virus do not alter the cellular response to serum addition or withdrawal [26, 27]. These observations indicate that established lymphoblastoid cell lines could be a suitable model to study the

influence of cell cycle-related events in the pathogenesis of AD.

We have previously reported that 15d-PGJ₂ inhibited the serum-enhanced cell proliferation of lymphoblasts from AD patients, by blocking the critical events for G₁/S transition [28]. The cyclopentenone partially inhibited phosphorylation of retinoblastoma protein (pRb) and up-regulated the levels of the cyclin-dependent kinase (CDK) inhibitor p27. This work was undertaken to further study the mechanism(s) involved in 15d-PGJ₂-induced increased levels of p27 protein in AD lymphoblasts. Our results suggest that 15d-PGJ₂ blockade of Ca²⁺/CaM-mediated overactivation of PI3K/Akt in AD cells is an important part of the mechanism by which the cyclopentenone regulates the expression levels of p27 and cell cycle progression in AD lymphoblasts. We report here that 15d-PGJ₂ appears to impair the binding of CaM to the p85 regulatory subunit of PI3K, thereby decreasing PI3K/Akt activation. This effect of the cyclopentenone results in reduced phosphorylation and degradation, as well as nuclear retention of p27 protein.

Materials and methods

Materials

All components for cell culture were obtained from Invitrogen (Carlsbad, CA). The kinases inhibitors Ly294002, SP600125, PD98059, and 15d-PGJ₂ were obtained from Calbiochem (Darmstadt, Germany). 9,10-Dihydro-15d-PGJ₂ was from Cayman Chemical (Ann Arbor, MI). Radioactive compounds were purchased from Amersham (Uppsala, Sweden). Polyvinylidene fluoride (PVDF) membranes for Western blots were purchased from Bio-Rad (Richmond, CA). Rabbit polyclonal antibodies (pAbs) against human phospho-Akt (Ser473), phospho-ERK1/2, total ERK1/2 and total JNK were obtained from Cell Signaling (Beverly, MA) and phospho-JNK was from Promega (Fitchburg, WI). Mouse monoclonal antibody anti-human lamin B1 (sc-20682) and anti-human PI3K p85 α (sc-1637) and pAbs such as rabbit anti-human p27 (sc-528), rabbit anti-human phospho-p27 (Thr187) (sc-16324-R), rabbit anti-human CDK2 (sc-748), rabbit anti-human ubiquitin (sc-913), rabbit anti-human pRb (sc-50), rabbit anti-human SKP2 (sc-7164), rabbit anti-human CaM I (FL-149) and goat anti-human total-Akt (sc-1618) were from Santa Cruz Biotechnologies (Santa Cruz, CA). The enhanced chemiluminescence (ECL) system was from Amersham. MG132 and MTT [3-(4,5-dimethylthiazol-2-yl)-2,5-diphenyltetrazolium bromide], histone H1, anti- β -actin, anti- α -tubulin antibodies were obtained from

Sigma Aldrich (Alcobendas, Spain). All other reagents were of molecular grade. 15d-PGJ₂ and MG132 were dissolved in dimethyl sulfoxide (Me₂SO). The final concentration of Me₂SO was 0.1 % in the culture medium.

Cell lines

Twenty patients diagnosed in the department of Neurology of the University Hospital Doce de Octubre (Madrid, Spain) with probable Alzheimer according to NINCDS-ADRDA (National Institute of Neurological and Communicative Diseases and Stroke-Alzheimer's Disease and Related Disorders Association) criteria were used in this study. The average age of onset of the disease was 74±2 years. A group of 20 non-demented age-matched individuals was used as control. In all cases, peripheral blood samples were taken after written informed consent of the patients or their relatives.

Establishment of LCLs was performed in our laboratory as previously described [29] by infecting peripheral blood lymphocytes with the EBV [30]. Cells were grown in suspension in T flasks in an upright position, in approximately 10 ml RPMI 1640 (Gibco, BRL) medium that contained 2 mM L-glutamine, 100 µg/ml penicillin/streptomycin and, unless otherwise stated, 10 % (v/v) fetal bovine serum (FBS) and maintained in a humidified 5 % CO₂ incubator at 37°C. Fluid was routinely changed every 2 days by removing the medium above the settled cells and replacing it with an equal volume of fresh medium.

Determination of cell proliferation

Proliferation was determined either by cell counting in a Neubauer chamber, or by using the MTT assay. This assay is based on the cleavage of 3-(4,5-dimethylthiazol-2-yl)-2,5 diphenyltetrazolium bromide by mitochondrial dehydrogenase in viable cells [31]. Potential toxicity of the reagents used was routinely checked by trypan blue exclusion under inverted phase-contrast microscopy.

Cell cycle analysis

Exponentially growing cultures of cell lines were seeded at an initial concentration of 1×10⁶ cells/ml. Cell cycle analysis was performed using a standard method [32]. Cells were fixed in 75 % ethanol for 1 h at room temperature. Subsequent centrifugation of the samples was followed by incubation of cells in PBS containing 1 µg/ml of RNase at room temperature for 20 min and staining with propidium iodide (PI; 25 µg/ml). Cells were analyzed in an EPICS-XL cytofluorimeter (Coulter Científica, Móstoles, Spain). Estimates of cell cycle phase distributions were

obtained by computer analysis of DNA content distributions.

Proteasome activity assay

The proteasome activity assay was performed in total cell extracts from control and AD lymphoblasts incubated in the absence or in the presence of 1 µM MG132 for 24 h. To measure the proteasome chymotrypsin peptidase activity, 10 µg protein extract was mixed with 300 µl reaction buffer containing 20 mM HEPES, 0.5 mM EDTA pH 8.0, 0.035 % SDS, and 20 µM succinyl-Leu-Leu-Val-Try-7-amido-4-methylcoumarin at 37°C for 90 min. Substrate hydrolysis was measured by monitoring the release of Try-7-amido-4-methylcoumarin using a spectrofluorometer (excitation at 370 nm, emission at 460 nm) as described [33].

Immunological analysis

Cell extracts. To prepare whole cell extracts, cells were harvested, washed in PBS and then lysed in ice-cold lysis buffer (50 mM Tris pH 7.4, 150 mM NaCl, 50 mM NaF, 1 % Nonidet P-40), containing 1 mM sodium orthovanadate, 1 mM PMSF, 1 mM sodium pyrophosphate and protease inhibitor Complete Mini Mixture (Roche, Mannheim).

Cytosolic and nuclear proteins were differentially extracted by lysing cells in ice-cold hypotonic buffer (10 mM HEPES, pH 7.9, 10 mM KCl, 0.1 mM EDTA, 0.1 mM EGTA, 1 mM DTT) containing 1 mM sodium orthovanadate, 1 mM PMSF, 1 mM sodium pyrophosphate, and protease inhibitor mixture. After extraction on ice for 15 min, 0.5 % Nonidet P-40 was added, and the lysed cells centrifuged at 4000 rpm for 10 min. Supernatants containing cytosolic proteins were centrifuged at 13 000 rpm for 10 min. Nuclei were washed twice with the hypotonic buffer, and then lysed in hypertonic buffer (20 mM HEPES, pH 7.9, 0.4 M NaCl, 1 mM EDTA, 1 mM EGTA, 1 mM DTT) containing 1 mM sodium orthovanadate, 1 mM PMSF, 1 mM sodium pyrophosphate and protease inhibitor mixture. After extraction on ice for 30 min, the samples were centrifuged at 15 000 rpm for 15 min at 4°C. Antibodies to α-tubulin and to lamin B1 were used to assess the purity of the fractions.

The protein content of the extracts was determined by the Bio-Rad protein assay kit (Bio-Rad Laboratories).

Western blot analysis. From the whole cell extracts, 50–100-µg samples were fractionated on a SDS-polyacrylamide gel, and transferred to PVDF membrane (Immobilon-P). The amount of protein and the integrity of transfer were verified by staining with

Ponceau-S solution (Sigma). The filters were then blocked with non-fat milk and incubated, overnight at 4°C, with primary antibodies at the following dilutions: 1:500 anti-p27, 1:500 anti-phospho p27, 1:1000 anti-SKP2, 1:500 anti-ubiquitin, 1:1000 anti-phospho Akt, 1:1000 anti-Akt, 1:2000 anti-β-actin, 1:2000 anti-α-tubulin and 1:1000 anti-lamin B1. Signals from the primary antibodies were amplified using species-specific antisera conjugated with horseradish peroxidase (Sigma) and detected with a chemiluminescent substrate detection system ECL (Amersham). Blots were stripped and reprobbed with anti-β-actin as a protein-loading control. The relative protein levels were determined by scanning the bands with a GS-800 imaging densitometer provided with the Quantity One 4.3.1. software from Bio-Rad, normalized by that of β-actin.

Immunoprecipitation and cyclin E/CDK2 kinase assay

Lymphoblasts from control and AD individuals were seeded at an initial cell density of 1×10^6 cells/ml and incubated for 24 h. Protein extracts (500 μg) were incubated with an antibody against CDK2 for 2 h at 4°C, followed by an incubation with 20 μl protein G-Sepharose for 2 h. Samples were washed in kinase buffer (50 mM KCl, 8 mM MgCl₂, 1 mM DTT, 3 mM ATP, 50 mM HEPES, pH 7.4). The immune complexes were resuspended in 40 μl kinase buffer containing histone H1 (0.2 μg/μl). [γ -³²P]ATP (10 μCi) was added, and after shaking for 1 h at 37°C, the reaction was stopped by addition of 10 μl 6× SDS sample buffer. After boiling, the samples were resolved by SDS-PAGE on a 12% gel and the phosphorylated histone H1 was visualized by autoradiography. The amounts of histone H1 were detected by gel staining with Coomassie.

Co-immunoprecipitation assays

Lymphoblasts from AD individuals were seeded at an initial cell density of 1×10^6 cells/ml and incubated for 24 h. Protein extracts (600 μg) were subjected to immunoprecipitation overnight at 4°C with an anti-p85 monoclonal antibody in the presence of 0.1 mM CaCl₂ or 2 mM EGTA. Samples were incubated then with protein G for 2 h at 4°C. Immunocomplexes were washed three times with ice-cold lysis buffer containing CaCl₂ or EGTA, suspended with sample buffer, boiled, resolved by SDS-PAGE, and transferred onto PVDF Immobilon-P transfer membrane filters. Blots were probed with an anti-CaM pAb. Membranes were reprobbed with the anti-p85 antibody to check for equal immunoprecipitation efficiency.

Confocal laser scanning microscopy

Lymphoblasts from AD individuals were seeded at an initial density of 1×10^6 cells/ml and incubated for 24 h in the absence or in the presence of 2.5 μM 15d-PGJ₂. Cells were harvested, washed in PBS and fixed in freshly prepared 4% paraformaldehyde in PBS for 30 min at room temperature. After two washes with PBS containing 3 μg/ml BSA, cells (approximately 10 000) were plated onto 0.1% poly-L-lysine-coated glass slides and allowed to adhere by spinning at 700 rpm for 7 min. Cells were permeabilized and blocked with PBS containing 0.2% Triton X-100 and 10% normal goat serum (NGS) for 1 h. Cells were incubated overnight with anti-p27 (1:50), washed, and incubated with Alexa Fluor 488-conjugated secondary antibody (1:200) for 1 h at room temperature. Samples were subsequently washed three times in PBS and mounted in Vectashield® Mounting Medium with DAPI (Vector Labs, UK) and visualized on confocal microscope (Leica DMRE2, Heidelberg, Germany).

Statistical analysis

Unless otherwise stated, all data represent means ± SE. Statistical analysis was performed on the Data Desk package (version 4.0) for Macintosh. Statistical significance was estimated by the Student's *t*-test or, when appropriated, by analysis of variance (ANOVA) followed by the Fischer's LSD test for multiple comparisons. Differences were considered significant at a level of $p < 0.05$.

Results

Effects of 15d-PGJ₂ on cell proliferation

It was previously reported that 15d-PGJ₂ has an anti-proliferative effect on lymphoblasts from AD patients associated with altered control of G₁/S transition and accumulation of p27 protein [28]. For this reason, we first tried to elucidate the effects of 15d-PGJ₂ treatment on the phosphorylation status of the pRb and on the kinase activity of cyclin E/CDK2 complex, the key regulators of transition from G₁ phase of the cell cycle to S phase. Figure 1A shows a time course analysis of the effect of 15d-PGJ₂ on rates of proliferation of control and AD lymphoblasts following serum stimulation. It is shown, in agreement with previous results [28], that AD cells proliferate at a higher rate than control cells (Fig. 1A). Addition of 15d-PGJ₂ had no effect on control cells, but significantly reduced the enhanced proliferative activity of AD cells (Fig. 1A). The effect of 15d-PGJ₂ reducing total cell number in AD cultures is not due to increased cell death. A comparative analysis, by flow cytometry, of cell cycle status of control and AD cells following treatment

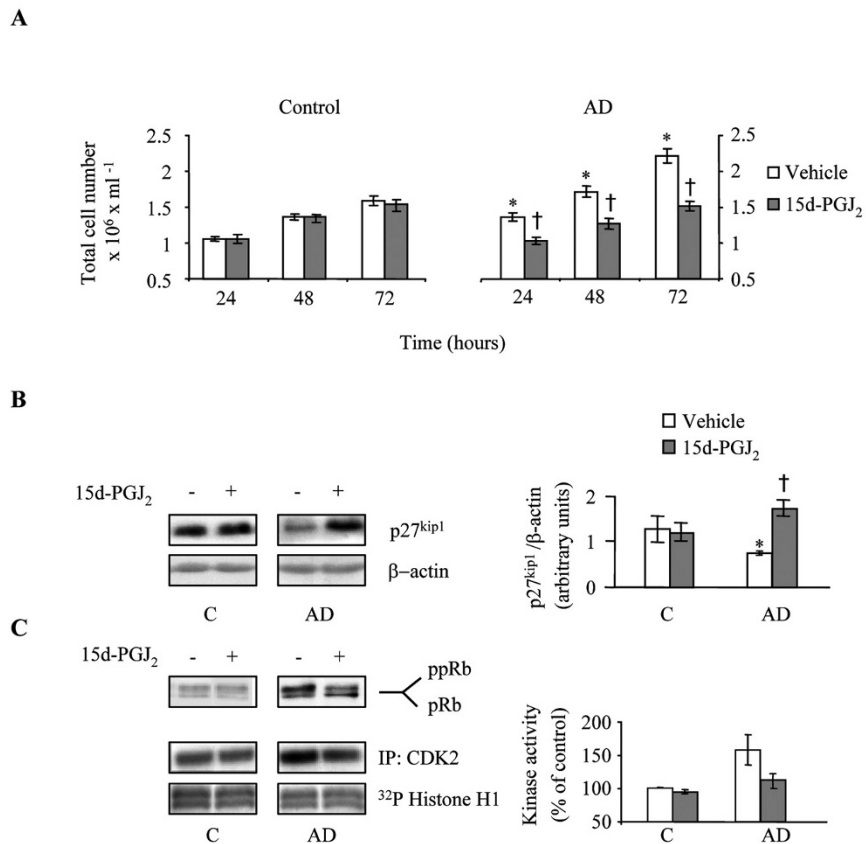


Figure 1. Effects of 15-deoxy- $\Delta^{12,14}$ -prostaglandin J₂ (15d-PGJ₂) on cell proliferation, p27 content, and phosphorylation status of retinoblastoma protein (pRb), and cyclin E/CDK2 kinase activity in control and lymphoblasts from Alzheimer's disease (AD) patients. (A) Lymphoblasts from control and AD subjects were seeded at an initial density of 1×10^6 /ml and incubated for 72 h in the absence or in the presence of 2.5 μ M 15d-PGJ₂. Aliquots were taken each day for cell enumeration. Values shown are the mean \pm SE for seven to fourteen experiments carried out with cells derived from different individuals. * $p < 0.01$ significantly different from control cells, † $p < 0.01$ significantly different from untreated AD lymphoblasts. (B) Whole cell extracts were prepared at 24 h after seeding, and immunoblotted as described in Materials and methods with anti-p27 antibody. A representative immunoblot is shown. Band intensity was measured and normalized by that of β -actin. * $p < 0.05$ significantly different from control cells, † $p < 0.05$ significantly different from untreated AD lymphoblasts. (C) Hypo- and hyper-phosphorylated pRb (ppRb) levels were determined by Western blot in cell extracts prepared 24 h after serum stimulation. Representative Western blots are presented. Immunoprecipitates obtained with anti-CDK2 antibody were assayed for kinase activity using histone H1 as substrate. Phosphorylated histone H1 was visualized using autoradiography. Levels of histone H1 were determined by gel staining with Coomassie. A representative experiment is shown, while below the densitometric analysis is presented. Data shown represent the mean \pm SE for four different experiments.

with 15d-PGJ₂ revealed that at the concentration of the drug used, there was no evidence of apoptosis/necrosis in either control or AD cell lines, since a subdiploid pre G₀/G₁ peak was not detected (not shown). As expected, the 15d-PGJ₂-induced inhibition of cell proliferation was accompanied by an accumulation of the CDKi p27 (Fig. 1B). 15d-PGJ₂ inhibited the serum-mediated enhanced cyclin E/CDK2-associated kinase activity in AD cells, and partially blocked pRb phosphorylation (Fig. 1C). Figure 2A shows that the effect of 15d-PGJ₂ inhibiting cell proliferation in AD lymphoblasts is reversible. For these experiments, lymphoblasts from AD patients were incubated in the absence and in the presence of 15d-PGJ₂ for 24 h, then, the medium was

changed and cells were enumerated every day. After 15d-PGJ₂ removal, the kinetics of cell proliferation was back to normal (Fig. 2A). As shown in Figure 2B, p27 levels decreased progressively, returning to basal levels following 15d-PGJ₂ withdrawal.

p27 accumulation is due to increased protein half-life in 15d-PGJ₂-treated cells

To determine if the increase in p27 protein following 15d-PGJ₂ treatment resulted from altered protein half-life, AD cells were incubated with and without 15d-PGJ₂ for 24 h at which time cells were treated with cycloheximide to block *de novo* protein synthesis. p27 levels were then determined by Western blot analysis in cells harvested at various time points after

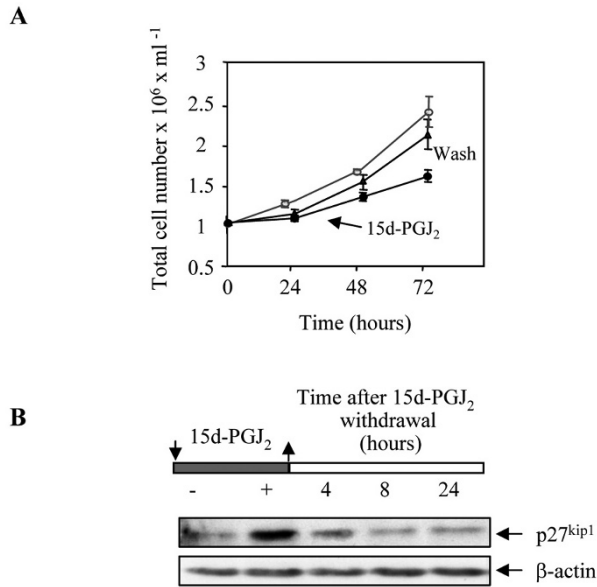


Figure 2. 15d-PGJ₂ inhibition of the serum-mediated enhanced proliferation of AD lymphoblasts and increased p27 content are reversible. (A) Lymphoblasts from AD patients were incubated in triplicate in 24-well plates (2×10^6 /well) in the absence or in the presence of $2.5 \mu\text{M}$ 15d-PGJ₂ for 24 h; the medium was then changed and cells were enumerated every day thereafter. 15d-PGJ₂ was kept in one of the wells as control. Data shown are the mean \pm SE for four independent experiments. (B) Lymphoblasts from AD patients were incubated in the presence of $2.5 \mu\text{M}$ 15d-PGJ₂ for 24 h. After replacing the medium, cells were cultured for an additional period of 24 h. Cells were harvested at the time points indicated in the figure and p27 was detected by immunoblotting. A representative experiment is shown.

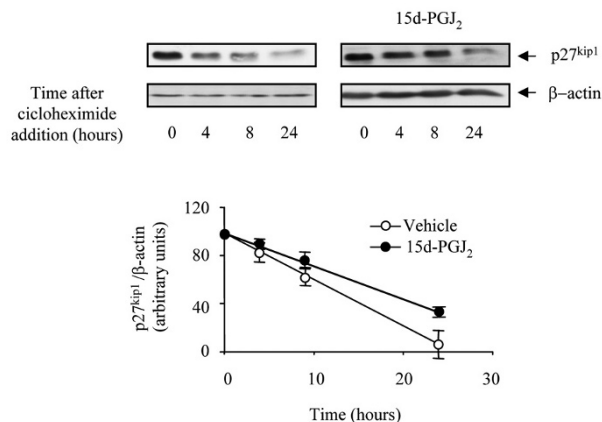


Figure 3. Effect of 15d-PGJ₂ on the half-life of p27 protein in AD lymphoblasts. Lymphoblasts from AD subjects were incubated for 24 h in RPMI medium containing 10% FBS, in the absence or in the presence of $2.5 \mu\text{M}$ 15d-PGJ₂ and then cycloheximide ($10 \mu\text{g/ml}$) was added. Cells were harvested 4, 8, and 24 h thereafter and p27 was detected by immunoblotting. The decay of the p27 signal is shown as a function of time post-cycloheximide addition. Linear regression curves were fitted to calculate the half-life of the protein using data from four different experiments.

cycloheximide addition. Figure 3 shows that p27 protein from 15d-PGJ₂-treated cells persisted longer than from untreated cells. The calculated half-life of p27 increased from 12 h to 22 h after 15d-PGJ₂ treatment.

Effects of 15d-PGJ₂ on p27 degradation

We next investigated whether the 15d-PGJ₂-mediated up-regulation of p27 protein in AD lymphoblasts was due to altered degradation of p27 protein, a process thought to take place in the proteasome [34]. p27 proteolysis is a three-step process that requires phosphorylation at Thr187, recognition by the F-box protein SKP2, ubiquitylation, and degradation by the 26S proteasome [34]. Figure 4 shows that 15d-PGJ₂ did not change the phosphorylation status of p27 in control cells, but abrogates the serum-induced increased levels of phospho-p27 (Thr187) in AD cells. There is a tight inverse relationship between levels of phospho-p27 and expression levels (Fig. 4). 15d-PGJ₂ treatment had no effect on the SKP2 content in either control or AD lymphoblasts. In addition, we did not find significant differences in the accumulation of ubiquitin-tagged proteins or in total proteasome activity between treated or untreated cells from control and AD patients (Fig. 5). Therefore, these results suggest that, by inhibiting cyclin E/CDK2 kinase activity, and decreasing Thr187 phosphorylation of p27, 15d-PGJ₂ abrogates targeting of SCF-ubiquitin E3 ligase and minimizes proteasome degradation of p27, thus increasing cellular content of p27.

Effects of 15d-PGJ₂ on PI3K/Akt-mediated down-regulation of p27 in AD lymphoblasts

We have shown previously [26] that serum-mediated enhanced cell proliferation, and decreased levels of p27 in AD cells, requires the activation of PI3K/Akt signaling pathway. Here, we show that the specific inhibitor of PI3K/Akt, Ly294002 mimicked the effects of 15d-PGJ₂ inhibiting cell proliferation and increasing the p27 content of AD cells (Fig. 6A and B). When cells were treated with Ly294002 and 15d-PGJ₂ at the same time, no further inhibition of cell growth nor increase of p27 were observed (Fig. 6A and B), suggesting no additive effects of these two drugs. In contrast to 15d-PGJ₂, the treatment of control cells with Ly294002 inhibited cell proliferation and increased the cellular content of p27 (Fig. 6A and B). The role of 15d-PGJ₂ on PI3K/Akt signaling pathway in control and AD lymphoblasts was assessed by monitoring the phosphorylation status of Akt, before and after 15d-PGJ₂ treatment, by Western blotting with a phospho-specific anti-Akt antibody. Figure 6C shows significant higher levels of phospho-Akt (Ser473) in AD cells compared with cells from age-

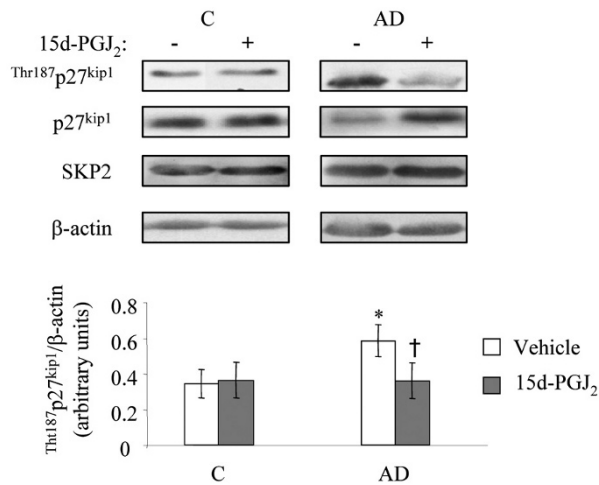


Figure 4. Effects of 15d-PGJ₂ on Thr¹⁸⁷p27 levels, and total p27 and SKP2 content in lymphoblasts from control and AD patients. Lymphoblasts were incubated in RPMI medium containing 10% FBS in the absence or in the presence of 2.5 μM 15d-PGJ₂ for 24 h. Whole cell extracts were immunoblotted with anti-phospho-p27 (Thr¹⁸⁷) and total p27, or with anti-SKP2. Representative immunoblots are presented. Densitometric data for Thr¹⁸⁷p27 protein are the mean ± SE for five experiments. **p*<0.05 significantly different from control cells, †*p*<0.05 significantly different from AD cells incubated in the absence of 15d-PGJ₂.

matched control individuals. Total content of Akt did not change. 15d-PGJ₂ prevented the serum-enhanced Akt phosphorylation in AD cells without affecting Akt activation in control cells (Fig. 6C). These results suggest that 15d-PGJ₂ prevents, rather than inhibits, overactivation of PI3K/Akt pathway in AD cells. Figure 6D shows that 15d-PGJ₂ did not affect either ERK1/2 or JNK activation in lymphoblasts from AD patients.

It has been shown that PI3K/Akt may also contribute to regulation of p27 content by altering the nucleocytoplasmic traffic of the protein [35, 36]. For these reasons, we studied whether 15d-PGJ₂ treatment induced changes in the subcellular localization of p27 in AD cells. To this end, AD lymphoblasts were incubated with either 15d-PGJ₂ or Ly294002 and either fractionated to enrich for nuclear or cytoplasmic proteins or processed for immunostaining and confocal laser scanning microscopy. The Western blotting analysis of cytoplasmic and nuclear proteins revealed that 15d-PGJ₂ induced an increase in the nuclear p27 content (Fig. 7A). Similar results were found when AD cells were treated with the PI3K/Akt inhibitor Ly294002 (Fig. 7A). The results of protein fractionation and immunoblotting were consistent with the effects of 15d-PGJ₂ in the localization of p27 determined by immunostaining (Fig. 7B).

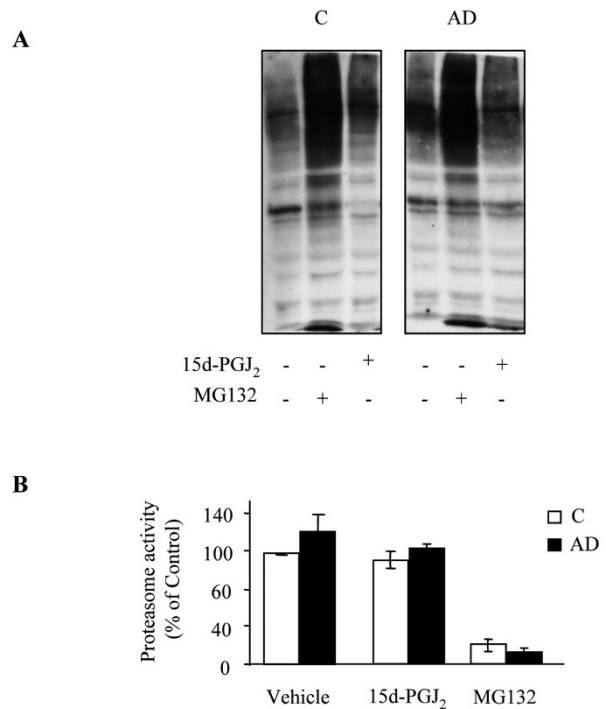


Figure 5. Effects of 15d-PGJ₂ on proteasome activity in control and AD lymphoblasts. (A) Lymphoblasts from control and AD patients were cultured for 48 h in the absence or in the presence of 2.5 μM 15d-PGJ₂ or 1 μM MG132 as positive control. Cells extracts were then subjected to immunoblot analysis using an antibody anti-ubiquitin. A representative experiment is shown. (B) Cell extracts were assayed for proteasome activity as described in Methods. Data shown represent the mean ± SE of six experiments carried out in cell lines from separate individuals in triplicate.

Effects of 15d-PGJ₂ on interaction of CaM and PI3K

The fact that 15d-PGJ₂ affects neither Akt phosphorylation nor p27 content in control cells suggests that the cyclopentenone is acting upstream of Akt. 15d-PGJ₂ somehow prevents the serum-mediated enhanced PI3K/Akt pathway in AD cells. Overactivation of PI3K/Akt signaling pathway in AD cells depends on Ca²⁺/CaM [26]. Moreover, it had been reported that CaM is able to associate with SH₂ domains in the 85-kDa regulatory subunit of PI3K (p85), thereby activating PI3K *in vitro*, and in intact cells [37, 38]. For this reason, we next explored whether 15d-PGJ₂ is able to blunt the potential interaction between PI3K and CaM. To this end, cell lysates from AD lymphoblasts were immunoprecipitated with the anti-p85 antibody. The immunoprecipitates were analyzed by Western blot, and the immunoblots were probed with an anti-CaM antibody. CaM was found to co-immunoprecipitate with p85 (Fig. 8A). As previously described [38], CaM and p85 interaction was found to be Ca²⁺ dependent (Fig. 8A). When 15d-PGJ₂ was added during the immunoprecipitation process, the association was strongly reduced,

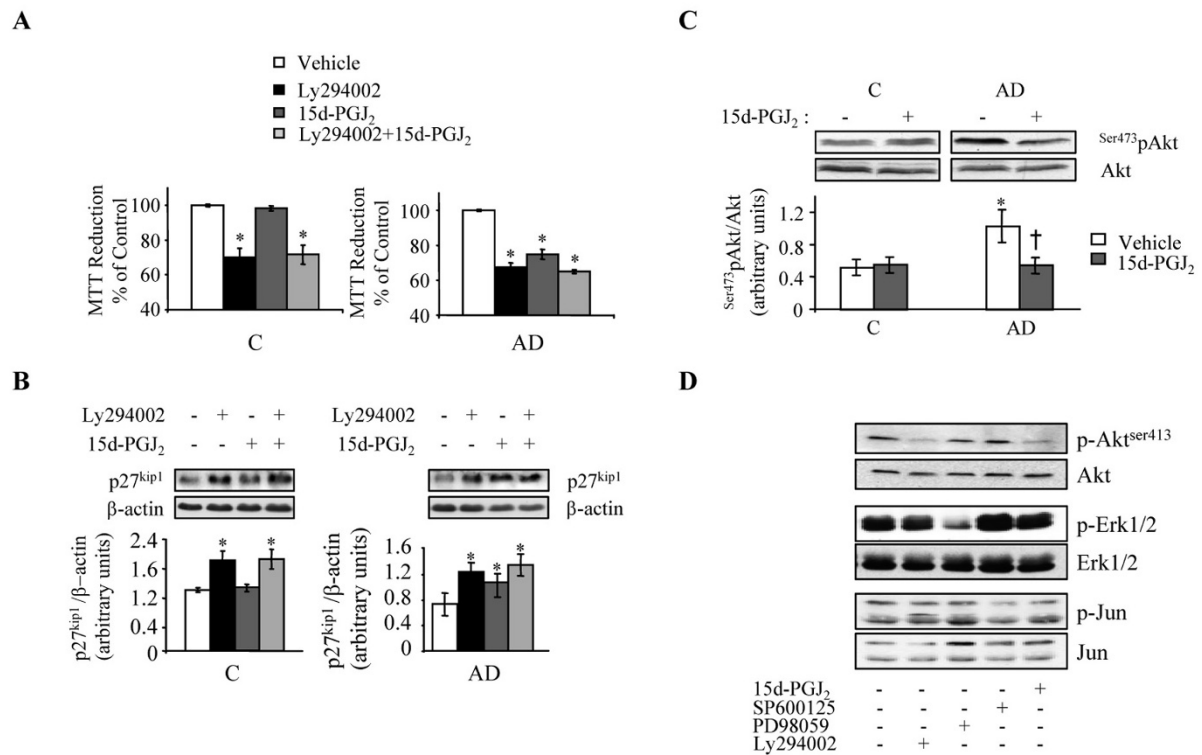


Figure 6. Effects of 15d-PGJ₂ on cell proliferation, p27 content and PI3K/Akt activation in control and lymphoblasts from AD patients. (A) Serum-deprived lymphoblasts from control and AD patients were preincubated for 30 min in the presence of 10 μM Ly294002 or 2.5 μM 15d-PGJ₂, and then stimulated by adding 10% FBS. Cell proliferation was assessed, after 24 h, by measuring the MTT reduction. Independent experiments with different cell lines were carried out in duplicate. Values shown are the mean ± SE for six experiments, and expressed as percentage of the value of untreated controls. **p* < 0.01 significantly different from untreated cells. (B) Whole cell extracts were subjected to immunoblotting. Representative immunoblots are presented. The immunoreactive bands were quantified by densitometric analysis. Results shown below are the mean ± SE of six determinations made in different experiments. **p* < 0.05 significantly different from untreated cells. (C) Cells were incubated as above. Whole cell lysates were immunoblotted with antibodies anti-phospho-Akt (Ser473) and total Akt. The densitometric data represent the mean ± SE for eight independent experiments. **p* < 0.05 significantly different from control cells; †*p* < 0.05 significantly different from untreated AD lymphoblasts. (D) Lymphoblasts from AD subjects were incubated in the absence or in the presence of 2.5 μM 15d-PGJ₂, 10 μM LY294002, 10 μM SP600125, or 20 μM PD98059 for 24 h. Whole cell extracts were subjected to immunoblotting with phospho-specific anti-Akt, anti-ERK1/2 and anti-JNK. The same membrane was reprobbed with antibodies to the corresponding total protein. Representative immunoblots from five experiments are presented.

indicating that 15d-PGJ₂ displaced CaM binding to PI3K *in vitro* (Fig. 8A). Therefore, these results suggest that treatment of AD cells with 15d-PGJ₂ could prevent CaM-mediated activation of PI3K.

The lack of effects of 15d-PGJ₂ in Akt phosphorylation in control cells suggest the existence of a threshold for CaM activation of PI3K. In consonance with this idea, we found increased expression levels of CaM in AD lymphoblasts compared with those observed in control cells (Fig. 8B).

Effects of 15d-PGJ₂ preventing activation of PI3K/Akt and up-regulation of p27 protein are unlikely to be mediated by PPAR_γ activation

We previously reported [28] that the anti-proliferative effect of 15d-PGJ₂ in human lymphoblasts is not dependent on PPAR_γ activation since it could not be blocked by the selective PPAR_γ antagonist GW9662,

and other PPAR_γ ligands did not mimic the effect of 15d-PGJ₂ on proliferation of AD cells. Data in Figure 9 confirm and extend our previous finding, by showing that cell proliferation (Fig. 9A), Akt phosphorylation and p27 levels are not affected in AD cells by 9,10-dihydro-15d-PGJ₂, an analog of 15d-PGJ₂ that was designed to retain PPAR_γ agonist activity and to be more resistant to metabolism [39] (Fig. 9B). These results also indicate that the α,β-unsaturated carbonyl group in the cyclopentenone ring of 15d-PGJ₂ is a requisite for the effects of 15d-PGJ₂ in AD cells.

Discussion

Prostaglandins are small lipid molecules that regulate numerous processes in the body and their biological effects have been the subject of intense research in

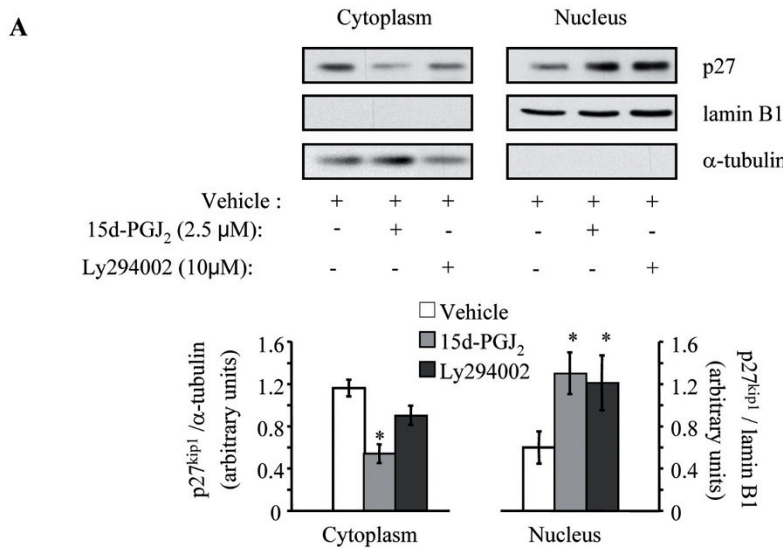
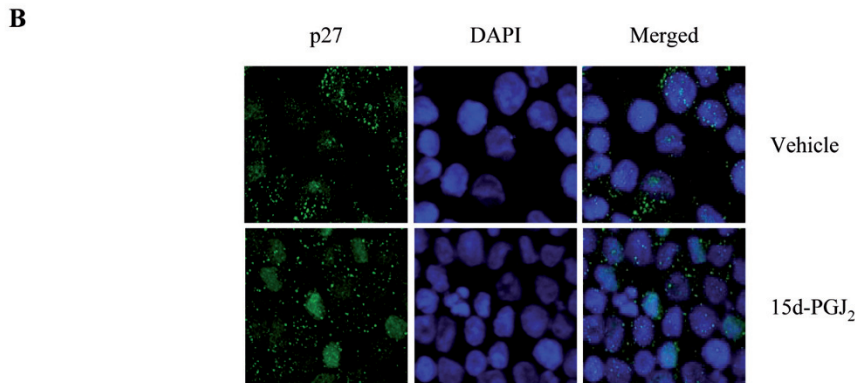


Figure 7. Effect of 15d-PGJ₂ on subcellular localization of p27. (A) Lymphoblasts from AD patients were incubated in the absence or in the presence of 2.5 μ M 15d-PGJ₂ or 10 μ M Ly294002 for 24 h, and fractionated to determine by immunoblot localization of p27. Antibodies to α -tubulin and to lamin B1 were used as control of purity and loading of cytoplasmic and nuclear protein extracts, respectively. Representative immunoblots are shown, whereas the densitometric analysis is presented below. Data represent mean \pm SE of eight experiments. * p <0.01 significantly different from untreated AD lymphoblasts. (B) p27 was studied by confocal laser scanning microscopy. Cells were stained with anti-p27 antibody followed by secondary antibody labeled with Alexa Fluor 488. DAPI was used for nuclear staining. Merged images depict a predominant nuclear localization for p27 in treated cells. Relative intensity was 0.2 ± 0.015 in untreated cells versus 1.2 ± 0.07 in the presence of 15 d-PGJ₂. Values are the mean \pm SE for 100 cells (magnification 63 \times).



recent years. The 15d-PGJ₂ is the end-product metabolite of PGD₂ and it is produced by a variety of cells, including mast cells, T cells, platelets, alveolar macrophages, and activated microglia. In monocytes/macrophages, 15d-PGJ₂ exerts an anti-inflammatory action due to the attenuation of the expression of various proinflammatory genes such as IL-1 and TNF, and the expression of effectors proteins such as cyclooxygenase-2, inducible nitric oxide synthase, and matrix metalloproteinases [40–42]. In addition, anti-neoplastic effects of 15d-PGJ₂ have been described in several cell types [8, 9]. Based on these observations, we hypothesized that the protective effects of anti-inflammatory drugs on AD progression could be related to their ability to regulate cell cycle events. It was reported that 15d-PGJ₂ is able to selectively blunt the serum-enhanced proliferation of immortalized lymphocytes from late-onset AD patients without affecting normal proliferative response of control cells

[28]. 15d-PGJ₂ inhibits cell cycle progression at the G₁/S checkpoint in AD lymphoblasts [28]. Our results show that treatment of AD cells with 15d-PGJ₂ decreased the activity of the cyclin E/CDK2 complex, apparently by up-regulating the levels of the CDKi p27 and partially blocked the enhanced phosphorylation of pRb protein induced by serum stimulation in AD lymphoblasts. The anti-proliferative effect of 15d-PGJ₂ was shown to be independent of PPAR γ activation [28]. In agreement with this observation, we report here the effects of 15d-PGJ₂ are not mimicked by the analog 9,10-dihydro-15d-PGJ₂ that retains PPAR γ agonist activity. This finding also indicates that the α,β -unsaturated carbonyl group in the cyclopentenone ring is required for the effects of 15d-PGJ₂ in AD lymphoblasts. PPAR γ -independent effects of 15d-PGJ₂ have been previously reported in other cell types, including cells of the nervous system [43, 44]. Several mechanisms have been implicated as

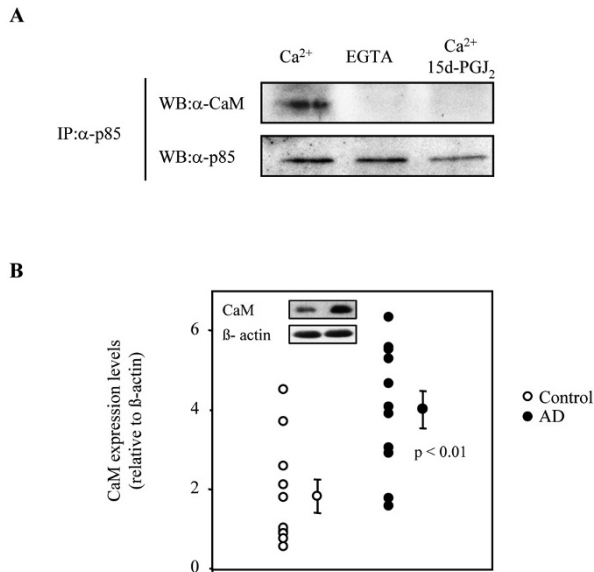


Figure 8. Effect of 15d-PGJ₂ on calmodulin (CaM) binding to p85 regulatory subunit of PI3K. (A) Lysates from AD lymphoblasts were immunoprecipitated with the anti-p85 antibody (α-p85) in the presence of 0.1 mM CaCl₂ or 2 mM EGTA, and 0.1 mM CaCl₂ plus 2.5 μM 15d-PGJ₂. Immunocomplexes were analyzed by Western blot with an anti-CaM antibody (α-CaM). Efficiency of p85 immunoprecipitation in the different conditions was checked by reprobing the membranes using the anti-α-p85 antibody. The experiment was repeated three times with similar results. (B) Scatter plot comparing CaM levels between control (open symbols) and AD lymphoblasts (filled symbols). Cells were seeded at an initial density of 1×10⁶/ml and cultured for 3 days in RPMI medium containing 10% FBS. Whole cell extracts were prepared thereafter, and immunoblotted with anti-α-CaM antibody. A representative immunoblot is shown in the inset. Band intensities were measured and normalized by that of β-actin. Statistical significance was determined by the *t*-test.

being responsible for the effects of 15d-PGJ₂ on the different cell types and these may partially explain its anti-neoplastic properties. Mediators of these actions include NF-κB inactivation [45], AP1 [38], reactive oxygen species [46], and the MAPK or PI3K/Akt pathways [47, 48]. It has been reported that the PPARγ-independent actions of 15d-PGJ₂ may be due to the reactive ring system [39]. Reduction of its double bond may impair significantly the ability of reacting covalently with nucleophile residues in cellular proteins.

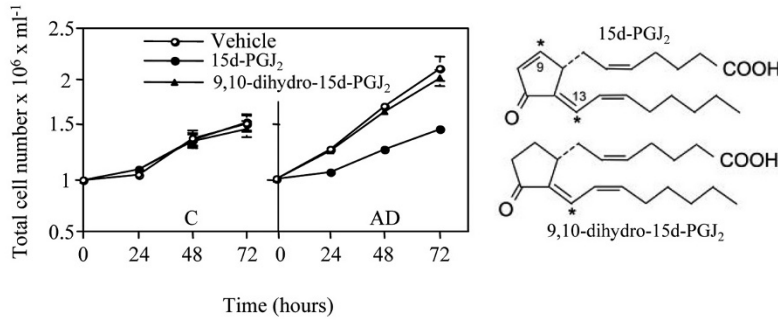
This study demonstrates that 15d-PGJ₂ blockade of PI3K/Akt overactivation is an important part of the mechanism by which the cyclopentenone regulates the expression levels of p27 and cell cycle progression in AD lymphoblasts. This asseveration finds support in the following observations: first, inhibition of PI3K/Akt by Ly294002 had effects similar to those of 15d-PGJ₂ on p27 content and cell proliferation, and second 15d-PGJ₂ reduced Akt activation in AD lymphoblasts. Activation of PI3K/Akt pathway has been previously

implicated in down-regulation of p27 levels in a number of cell types [49–51]. The molecular mechanisms involved in PI3K/Akt-mediated p27 regulation are not completely understood, but include modulation of transcription, protein degradation and subcellular localization of p27. Our data reveal that levels of p27 were post-translationally up-regulated by 15d-PGJ₂ by decreasing the rate of p27 degradation in the ubiquitin-proteasome pathway. The half-life of p27 after 15d-PGJ₂ treatment of AD cells is considerably lengthened, approaching values observed in lymphoblasts from control individuals [26]. The 15d-PGJ₂-mediated up-regulation of p27 protein correlated with inhibition of phosphorylation of p27 at Thr187 by the cyclin E/CDK2 complex, together with increased levels of p27 in the nucleus. The p27-specific F-box, protein SKP2, interacts with the C terminus of the phosphorylated protein in the cytosol. This association results in recruitment of p27 to the SCF core complex, thereby promoting its ubiquitination and degradation [52, 53]. Treatment of AD cells with 15d-PGJ₂ did not affect the expression levels of SKP2, the global proteasome activity or the accumulation of ubiquitin-tagged protein. These observations are in line with a recent report showing no differences in peripheral proteasome activity between control and AD lymphocytes [54].

The fact that 15d-PGJ₂ affects neither Akt phosphorylation nor p27 content in control cells suggests that the cyclopentenone is acting upstream of Akt. 15d-PGJ₂ somehow prevents the serum-mediated enhanced PI3K/Akt pathway in AD cells. We have recently reported that serum-mediated Akt activation in lymphoblasts from AD cells is Ca²⁺/CaM sensitive [26]. We report here that 15d-PGJ₂ is able to impair the binding of CaM to the 85-kDa regulatory subunit of PI3K (p85) *in vitro*. This mechanism could account for the decrease in Akt activation induced by 15d-PGJ₂ in AD cells, as it was previously demonstrated that CaM association with SH₂ domains in p85 leads to PI3K activation either *in vitro* or in intact cells [37, 38]. In addition, our results suggest the existence of a threshold for CaM to induce activation of PI3K/Akt pathway in human lymphocytes.

In summary, the present work indicates that 15d-PGJ₂ is able to suppress the Ca²⁺/CaM-enhanced activity of the PI3K/Akt signaling pathway in AD cells, leading to a significant increase in the levels of the CDKi p27, and thus inhibiting cell proliferation (Fig. 10). 15d-PGJ₂-mediated decrease of Akt activity impaired the increased phosphorylation of p27 at Thr187 and induced the retention of p27 in the nucleus, thus decreasing the cytosolic degradation of p27 by the proteasome.

A



B

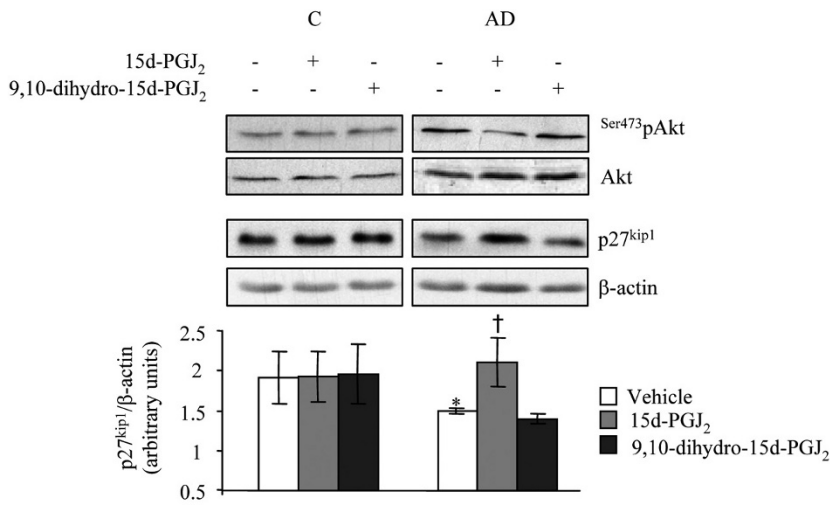
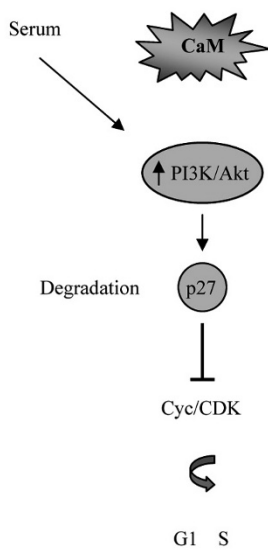


Figure 9. Effects of 15d-PGJ₂ and 9,10 dihydro-15d-PGJ₂ on cell proliferation, p27 content and PI3K/Akt activity in control and AD lymphoblasts. (A) Serum-deprived lymphoblasts from control and AD patients were pre-incubated for 30 min in absence or in the presence 2.5 μM 15d-PGJ₂ or 9,10 dihydro-15d-PGJ₂, and then stimulated by adding 10% FBS and incubated for 72 h. Cells were enumerated each day. Data shown are the mean ± SE for three independent experiments. (B) Cells were harvested after 24 h of serum stimulation and p27 was detected by immunoblotting. Densitometric data for p27 are shown below. **p*<0.05 significantly different from control cells. †*p*<0.05 significantly different from untreated AD lymphoblasts. (C) Whole cell lysates were immunoblotted with antibodies anti-phospho-Akt (Ser473) and total Akt. A representative immunoblot is shown.

A



B

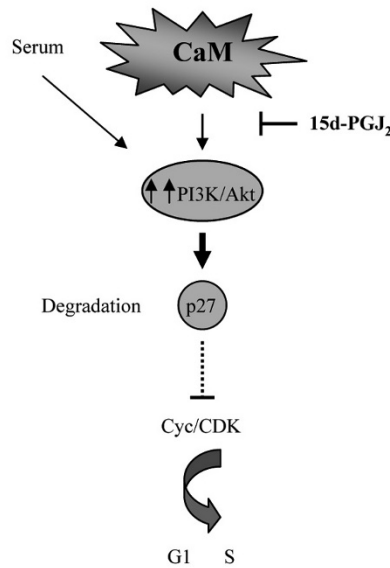


Figure 10. Diagram summarizing the role of 15d-PGJ₂ in preventing Ca²⁺/CaM-mediated over activation of PI3K/Akt in AD lymphoblasts. (A) In control cells, serum stimulation promotes proliferation by inducing PI3K/Akt activity, which in turn, induced p27 degradation. (B) In AD cells, in absence of 15d-PGJ₂ increased levels of CaM synergy with serum stimulation and promote overactivation of PI3K/Akt leading to enhanced p27 degradation. Treatment of cells with 15d-PGJ₂ prevent CaM-dependent activation of PI3K/Akt, normalize p27 levels and blocked the serum-mediated enhanced proliferation.

Alterations in Akt activity [55], changes in the abundance of p27 [56], as well as changes in cyclin/CDK activity [57] have also been detected in AD brain, suggesting that peripheral cells from patients may be a potential useful surrogate for diagnosis, prognosis and therapeutic monitoring of AD. The alteration in both cyclin/CDK activity and CDKi content seems to contribute significantly to AD pathology since abnormal cyclin/CDK activity appears to correlate with enhanced tau phosphorylation and tangle formation [57]. Moreover, phosphorylated p27 (Thr187) shows considerable overlap with tau-positive neurofibrillary pathology in AD brains [58]. Although cyclopentenone prostaglandins cannot be considered inert compounds, our observation that 15d-PGJ₂ had no detectable effects in cell proliferation and signaling through PI3K/Akt in control cells, while it is capable of selectively suppress the serum-mediated enhanced activation of AD cells, indicates its potential benefit in a therapeutic setting.

Acknowledgements. This work has been supported by grants from Ministry of Education and Science (SAF2007–62405) and Fundación Eugenio Rodríguez Pascual. N.E. holds a fellowship of the JAE predoctoral program of the CSIC.

- 1 McGeer, P. L. and McGeer, E. G. (2007) NSAIDs and Alzheimer disease: Epidemiological, animal model and clinical studies. *Neurobiol. Aging* 28, 639–647.
- 2 McGeer, P. L., Rogers, J. and McGeer, E. G. (2006) Inflammation, anti-inflammatory agents and Alzheimer disease: The last 12 years. *J. Alzheimers Dis.* 9, 271–276.
- 3 Lehmann, J. M., Lenhard, J. M., Oliver, B. B., Ringold, G. M. and Kliewer, S. A. (1997) Peroxisome proliferator-activated receptors alpha and gamma are activated by indomethacin and other non-steroidal anti-inflammatory drugs. *J. Biol. Chem.* 272, 3406–3410.
- 4 Gilroy, D. W., Colville-Nash, P. R., Willis, D., Chivers, J., Paul-Clark, M. J. and Willoughby, D. A. (1999) Inducible cyclooxygenase may have anti-inflammatory properties. *Nat. Med.* 5, 698–701.
- 5 Zingarelli, B., Sheehan, M., Hake, P. W., O'Connor, M., Denenberg, A. and Cook, A. (2003) Peroxisome proliferator activator receptor-gamma ligands, 15-deoxy-12,14-prostaglandin J₂ and ciglitazone, reduce systemic inflammation in polymicrobial sepsis by modulation of signal transduction pathways. *J. Immunol.* 171, 6827–6837.
- 6 Ianaro, A., Ialenti, A., Maffia, P., Di Meglio, P., Di Rosa, M. and Santoro, M. G. (2003) Anti-inflammatory activity of 15-deoxy-12,14-PGJ₂ and 2-cyclopenten-1-one: Role of the heat shock response. *Mol. Pharmacol.* 64, 85–93.
- 7 Blanco, M., Moro, M. A., Davalos, A., Leira, R., Castellanos, M., Serena, J., Vivancos, J., Rodríguez-Yanez, M., Lizasoain, I. and Castillo, J. (2005) Increased plasma levels of 15-deoxydelta prostaglandin J₂ are associated with good outcome in acute atherothrombotic ischemic stroke. *Stroke* 36, 1189–1194.
- 8 Han, S. W., Greene, M. E., Pitts, J., Wada, R. K. and Sidell, N. (2001) Novel expression and function of peroxisome proliferator-activated receptor gamma (PPARgamma) in human neuroblastoma cells. *Clin. Cancer Res.* 7, 98–104.
- 9 Chaffer, C. L., Thomas, D. M., Thompson, E. W. and Williams, E. D. (2006) PPARgamma-independent induction of growth arrest and apoptosis in prostate and bladder carcinoma. *BMC Cancer* 6, 53.
- 10 Arendt, T. (2003) Synaptic plasticity and cell cycle activation in neurons are alternative effectors pathways: The 'Dr. Jekyll and Mr. Hyde concept' of Alzheimer's disease or the yin and yang of neuroplasticity. *Prog. Neurobiol.* 71, 83–248.
- 11 Herrup, K., Neve, R., Ackerman, S. L. and Copani, A. (2004) Divide and die: Cell cycle events as triggers of nerve cell death. *J. Neurosci.* 24, 9232–9239.
- 12 Nagy, Z. (2005) The last neuronal division: A unifying hypothesis for the pathogenesis of Alzheimer's disease. *J. Cell. Mol. Med.* 9, 531–541.
- 13 Neve, R. L. and McPhie, D. L. (2006) The cell cycle as therapeutic target for Alzheimer's disease. *Pharmacol. Ther.* 111, 99–113.
- 14 Nagy, Z. (2000) Cell cycle regulatory failure in neurones: Causes and consequences. *Neurobiol. Aging* 21, 761–769.
- 15 Casadesus, G., Zhu, X., Atwood, C. S., Webber, K. M., Perry, G., Bowen, R. L. and Smith, M. A. (2004) Beyond estrogen: Targeting gonadotropin hormones in the treatment of Alzheimer's disease. *Curr. Drug Targets CNS Neurol. Disord.* 3, 281–285.
- 16 Webber, K. M., Raina, A. K., Marlatt, M. W., Zhu, X., Prat, M. I., Morelli, L., Casadesus, G., Perry, G. and Smith, M. A. (2005) The cell cycle in Alzheimer disease: A unique target for neuropharmacology. *Mech. Ageing Dev.* 126, 1019–1025.
- 17 Huang, H. M., Martins, R., Gandy, S., Etcheberrigaray, R., Ito, E., Alkon, D. L., Blass, J. and Gibson, G. (1994) Use of cultured fibroblasts in elucidating the pathophysiology and diagnosis of Alzheimer's disease. *Ann. N. Y. Acad. Sci.* 747, 225–244.
- 18 Mecocci, P., Polidori, M. C., Ingegnì, T., Cherubini, A., Chionne, F., Cecchetti, R. and Senin, U. (1998) Oxidative damage to DNA in lymphocytes from AD patients. *Neurology* 51, 1014–1017.
- 19 Tatebayashi, Y., Takeda, M., Kashiwagi, Y., Okochi, M., Kurumadani, T., Sekiyama, A., Kanayama, G., Hariguchi, S. and Nishimura, T. (1995) Cell-cycle-dependent abnormal calcium response in fibroblasts from patients with familial Alzheimer's disease. *Dementia* 6, 9–16.
- 20 Nagy, Z. S., Combrinck, M., Budge, M. and McShane, R. (2002) Cell cycle kinesis in lymphocytes in the diagnosis of Alzheimer's disease. *Neurosci. Lett.* 317, 81–84.
- 21 Neitzel, H. (1986) A routine method for the establishment of permanent growing lymphoblastoid cell lines. *Hum. Genet.* 73, 320–326.
- 22 Beatty, P. R., Krams, S. M. and Martinez, O. M. (1997) Involvement of IL-10 in the autonomous growth of EBV-transformed B cell lines. *J. Immunol.* 158, 4045–4051.
- 23 Minami, R., Watanabe, Y., Kudoh, T., Suzuki, M., Oynagi, K., Orii, T. and Nakao, T. (1978) Lysosomal acid hydrolases in established lymphoblastoid cell lines transformed by Epstein-Barr virus, from patients with genetic lysosomal storage diseases. *Hum. Genet.* 44, 79–87.
- 24 de las Cuevas, N., Urcelay, E., Hermida, O. G., Saiz-Diaz, R. A., Bermejo, F., Ayuso, M. S. and Martín-Requero, A. (2003) Ca²⁺/calmodulin-dependent modulation of cell cycle elements pRb and p27kip1 involved in the enhanced proliferation of lymphoblasts from patients with Alzheimer dementia. *Neurobiol. Dis.* 13, 254–263.
- 25 de las Cuevas, N., Muñoz, U., Hermida, O. G. and Martín-Requero, A. (2005) Altered transcriptional regulators in response to serum in immortalized lymphocytes from Alzheimer's disease patients. *Neurobiol. Aging* 26, 615–624.
- 26 Muñoz, U., Bartolomé, F., Bermejo, F. and Martín-Requero, A. (2008) Enhanced proteasome-dependent degradation of the CDK inhibitor p27 (kip1) in immortalized lymphocytes from Alzheimer's dementia patients. *Neurobiol. Aging* 29, 1474–1484.
- 27 Bartolomé, F., de las Cuevas, N., Muñoz, U., Bermejo, F. and Martín-Requero, A. (2007) Impaired apoptosis in lymphoblasts from Alzheimer's disease patients: Cross-talk of Ca²⁺/calmodulin and ERK1/2 signaling pathways. *Cell. Mol. Life Sci.* 64, 1437–1448.

- 28 Muñoz, U., de las Cuevas, N., Bartolomé, F., Hermida, O. G., Bermejo, F. and Martín-Requero, A. (2005) The cyclopentenone 15-deoxy- $\Delta^{12,14}$ -prostaglandin J₂ inhibits G1/S transition and retinoblastoma protein phosphorylation in immortalized lymphocytes from Alzheimer's disease patients. *Exp. Neurol.* 195, 508–517.
- 29 Ibarreta, D., Urcelay, E., Parrilla, R. and Ayuso, M. S. (1998) Distinct pH homeostatic features in lymphoblasts from Alzheimer's disease patients. *Ann. Neurol.* 44, 216–222.
- 30 Koistinen, P. (1987) Human peripheral blood and bone marrow cell separation using density gradient centrifugation on Lymphoprep and Percoll in haematological diseases. *Scan. J. Clin. Lab. Invest.* 47, 709–714.
- 31 Mitsiades, N., Mitsiades, C. S., Poulaki, V., Chauhan, D., Richardson, P. G., Hideshima, T., Munshi, N., Treon, S. P. and Anderson, K. C. (2002) Biologic sequelae of nuclear factor-kappaB blockade in multiple myeloma: Therapeutic applications. *Blood* 99, 4079–4086.
- 32 Krishan, A. (1975) Rapid flow cytofluorometric analysis of mammalian cell cycle by propidium iodide staining. *J. Cell Biol.* 66, 188–193.
- 33 Dick, L. R., Cruikshank, A. A., Destree, A. T., Grenier, L., McCormack, T. A., Melandri, F. D., Nunes, S. L., Palombella, V. J., Parent, L. A., Plamondon, L. and Stein, R. L. (1997) Mechanistic studies on the inactivation of the proteasome by lactacystin in cultured cells. *J. Biol. Chem.* 272, 182–188.
- 34 Pagano, M., Tam, S. W., Theodoras, A. M., Beer-Romero, P., DelSal, G., Chau, V., Yew, P. R., Draetta, G. F. and Rolfe, M. (1995) Role of the ubiquitin-proteasome pathway in regulating abundance of the cyclin-dependent kinase inhibitor p27. *Science* 269, 682–685.
- 35 Shin, I., Yakes, F. M., Rojas, F., Shin, N.-Y., Bakini, A. V., Balsega, J. and Arteaga, C. L. (2002) PKB/Akt mediates cell-cycle progression by phosphorylation of p27^{Kip1} at threonine 157 and modulation of its cellular localization. *Nat. Med.* 8, 1145–1152.
- 36 Cappellini, A., Tabellini, G., Zwyer, M., Bortul, R., Tazzari, P. L., Billi, A. M., Fala, F., Cocco, L. and Martelli, A. M. (2003) The phosphoinositide 3-kinase/Akt pathway regulates cell cycle progression of HL60 human leukemia cells through cytoplasmic relocalization of the cyclin-dependent kinase inhibitor p27^{Kip1} and control of cyclin D1 expression. *Leukemia* 17, 2157–2167.
- 37 Joyal, J. L., Burks, D. J., Pons, S., Matter, W. F., Vlahos, C. J., White, M. F. and Sacks, D. B. (1997) Calmodulin activates phosphatidylinositol 3-kinase. *J. Biol. Chem.* 272, 28183–28186.
- 38 Perez-Garcia, M. J., Cena, V., de Pablo, Y., Llovera, M., Comella, J. X. and Soler, R. M. (2004) Glial cell line-derived neurotrophic factor increases intracellular calcium concentration. Role of calcium/calmodulin in the activation of the phosphatidylinositol 3-kinase pathway. *J. Biol. Chem.* 279, 6132–6142.
- 39 Paumi, C. M., Wright, M., Townsend, A. J. and Morrow, C. S. (2003) Multidrug resistance protein (MRP) 1 and MRP3 attenuate cytotoxic and transactivating effects of the cyclopentenone prostaglandin, 15-deoxy-12,14-prostaglandin J₂ in MCF7 breast cancer cells. *Biochemistry* 42, 5429–5437.
- 40 Ricote, M., Li, A. C., Willson, T. M., Kelly, C. J. and Glass, C. K. (1998) The peroxisome proliferator-activated receptor-gamma is a negative regulator of macrophage activation. *Nature* 391, 79–82.
- 41 Marx, N., Schönbeck, U., Lazar, M. A., Libby, P. and Plutzky, J. (1998) Peroxisome proliferator-activated receptor gamma activators inhibit gene expression and migration in human vascular smooth muscle cells. *Circ. Res.* 83, 1097–1103.
- 42 Sawano, H., Haneda, M., Sugimoto, T., Inoki, K., Koya, D. and Kikkawa, R. (2002) 15-Deoxy-delta12,14-prostaglandin J₂ inhibits IL-1beta-induced cyclooxygenase-2 expression in mesangial cells. *Kidney Int.* 61, 1957–1967.
- 43 Boyault, S., Simonin, M. A., Bianchi, A., Compe, E., Liagre, B., Mainard, D., Becuwe, P., Dauca, M., Netter, P., Terlain, B. and Bordji, K. (2001) 15-Deoxy-delta 12,14-PGJ₂, but not troglitazone, modulates IL-1beta effects in human chondrocytes by inhibiting NF-kappaB and AP-1 activation pathways. *FEBS Lett.* 501, 24–30.
- 44 Janabi, N. (2002) Selective inhibition of cyclooxygenase-2 expression by 15-deoxy-delta (12,14)(12,14)-prostaglandin J(2) in activated human astrocytes, but not in human brain macrophages. *J. Immunol.* 168, 4747–4755.
- 45 Cernuda-Morollón, E., Pineda-Molina, E., Cañada, F. J. and Perez-Sala, D. (2001) 15-Deoxy-delta 12,14-prostaglandin J₂ inhibition of NF-kappaB-DNA binding through covalent modification of the p50 subunit. *J. Biol. Chem.* 276, 35530–35536.
- 46 Lennon, A. M., Ramaugé, M., Dessouroux, A. and Pierre, M. (2002) MAP kinase cascades are activated in astrocytes and preadipocytes by 15-deoxy-12,14-prostaglandin J₂ and the thiazolidinedione ciglitazone through peroxisome proliferator activator receptor-independent mechanisms involving reactive oxygenated species. *J. Biol. Chem.* 277, 29681–29685.
- 47 Harris, S.G., Smith, R. S. and Phipps, R. P. (2002) 15-Deoxy-delta 12,14-PGJ₂ induces IL-8 production in human T cells by a mitogen-activated protein kinase pathway. *J. Immunol.* 168, 1372–1379.
- 48 Giri, S., Rattan, R., Singh, A. K. and Singh, I. (2004) The 15-deoxy-delta12,14-prostaglandin J2 inhibits the inflammatory response in primary rat astrocytes *via* down-regulating multiple steps in phosphatidylinositol 3-kinase-Akt-NF-kappaB-p300 pathway independent of peroxisome proliferator-activated receptor gamma. *J. Immunol.* 173, 5196–5208.
- 49 Li, D. M. and Sun, H. (1998) PTEN/MMAC1/TEP1 suppresses the tumorigenicity and induces G₁ cell cycle arrest in human glioblastoma cells. *Proc. Natl. Acad. Sci. USA* 95, 15406–15411.
- 50 Radu, A., Neubauer, V., Akagi, T., Hanafusa, H. and Georgescu, M. M. (2003) PTEN induces cell cycle arrest by decreasing the level and nuclear localization of cyclin D1. *Mol. Cell. Biol.* 23, 6139–6349.
- 51 Liang, J. and Slingerland, J. M. (2003) Multiple roles of the PI3K/PKB (Akt) pathway in cell cycle progression. *Cell Cycle* 2, 339–345.
- 52 Carrano, A.C., Eytan, E., Hershko, A. and Pagano, M. (1999) SKP2 is required for ubiquitin-mediated degradation of the CDK inhibitor p27. *Nat. Cell Biol.* 1, 193–199.
- 53 Nakayama, K., Nagahama, H., Minamishima, Y. A., Matsumoto, M., Nakamichi, I., Kitagawa, K., Shirane, M., Tsunematsu, R., Tsukiyama, T., Ishida, N., Kitagawa, M., Nakayama, K. and Hatakeyama, S. (2000) Targeted disruption of Skp2 results in accumulation of cyclin E and p27 (Kip1), polyploidy and centrosome overduplication. *EMBO J.* 19, 2069–2081.
- 54 Blandini, F., Sinforiani, E., Pacchetti, C., Samuele, A., Bazzini, E., Zangaglia, R., Nappi, G. and Martignoni, E. (2006) Peripheral proteasome and caspase activity in Parkinson disease and Alzheimer disease. *Neurology* 66, 529–534.
- 55 Rickle, A., Bogdanovic, N., Volkman, I., Winblad, B., Ravid, R. and Cowburn, R. F. (2004) Akt activity in Alzheimer's disease and other neurodegenerative disorders. *Neuroreport* 15, 955–959.
- 56 Griffin, R. J., Moloney, A., Kelliher, M., Johnston, J. A., Ravid, R., Dockery, P., O'Connor, R. and O'Neill, C. (2005) Activation of Akt/PKB, increased phosphorylation of Akt substrates and loss and altered distribution of Akt and PTEN are features of Alzheimer's disease pathology. *J. Neurochem.* 93, 105–117.
- 57 McShea, A., Harris, P. L. R., Webster, K. R., Wahl, A. P. and Smith, M. A. (1997) Abnormal expression of cell cycle regulators P16 and CDK4 in Alzheimer's disease. *Am. J. Pathol.* 150, 1933–1939.
- 58 Ogawa, O., Lee, H. G., Zhu, X., Raina, A., Harris, P. L., Castellani, R. J., Perry, G. and Smith, M. A. (2003) Increased p27, an essential component of cell cycle control, in Alzheimer's disease. *Aging Cell* 2, 105–110.